

Early Estimation of Microlensing Event Magnifications

Michael D. Albrow

*Department of Physics and Astronomy, University of Canterbury, Private Bag 4800,
Christchurch, New Zealand*

Michael.Albrow@canterbury.ac.nz

ABSTRACT

Gravitational microlensing events with high peak magnifications provide a much enhanced sensitivity to the detection of planets around the lens star. However, estimates of peak magnification during the early stages of an event by means of χ^2 minimization frequently involve an overprediction, making observing campaigns with strategies that rely on these predictions inefficient.

I show that a rudimentary Bayesian formulation, incorporating the known statistical characteristics of a detection system, produces much more accurate predictions of peak magnification than χ^2 minimisation. Implementation of this system will allow efficient follow-up observing programs that focus solely on events that contribute to planetary abundance statistics.

Subject headings: gravitational lensing — methods: data analysis

1. Introduction

Following the suggestion of Paczyński (1986), several collaborations, notably MACHO and EROS, began to search for gravitational microlensing towards the Magellanic Clouds as an indicator of compact objects in the halo of the Milky Way (Alcock et al. 1993; Aubourg et al. 1993). At about the same time, the OGLE collaboration began a survey in the direction of the Galactic bulge (Udalski et al. 1992, 1993). It was soon found that a much higher event rate occurred in fields towards the Galactic bulge relative to the rate towards the Magellanic Clouds (Udalski et al. 1994a; Alcock et al. 1995, 1997a). Since 1990, approximately 1000 such events have been detected (Alcock et al. 2000; Udalski et al. 2000).

Several groups including PLANET (Probing Lensing Anomalies NETwork, Albrow et al. 1998, 2001; Dominik et al. 2002; Gaudi et al. 2002), MPS (Microlensing Planet Search, Rhie et al. 1999) and μ FUN (Microlensing Follow-Up Network, Yoo et al. 2004) monitor events

much more intensively than the survey groups in order to identify anomalous behavior that can signal the presence of a planet associated with the lens star. High-magnification events in particular (those with $A_0 \gtrsim 10$) attract the attention of follow-up groups since it is these that are most likely to give detectable planetary signals (Griest & Safizadeh 1998; Gaudi, Naber & Sackett 1998). In addition, for high magnification events the angular size of the source star may be non-negligible in comparison to the lens-source angular separation. In these cases the lightcurves of the events can provide the possibility to determine the lens-source relative proper motion (Gould 1994; Alcock et al. 1997b) and atmospheric properties of the source (Heyrovský 2003).

In the first years of operation, when microlensing alerts came primarily from the MA-CHO collaboration, detected event rates were low enough that PLANET could monitor almost all potentially interesting events with ease. For the last two years (the 2002 and 2003 Bulge seasons), this has not been the case, due to the much improved alert rate since the advent of the OGLE III early warning system (EWS), <http://www.astrouw.edu.pl/ogle/ogle3/ews/ews.html> (Udalski et al. 1994b; Udalski 2003). In excess of 400 events were alerted by the EWS in each of these years. In addition, approximately 75 events were alerted in 2003 by the MOA collaboration (Bond et al. 2002) although some of these were duplicates of EWS events. We are now in an era in which a careful selection of events is necessary to optimize planet detection and exclusion productivity. For this reason, follow-up groups require accurate predictions of eventual maximum amplifications in the early days following a detection. For the remainder of this paper I will focus exclusively on events detected by the OGLE III EWS.

2. Fitting microlensing lightcurves

Most microlensing events are well fitted by a point-source point-mass-lens (PSPL) model for the magnification $A(t)$ at time t ,

$$A(u) = \frac{u^2 + 2}{u\sqrt{u^2 + 4}}, \quad (1)$$

$$u(\tau) = \sqrt{u_0^2 + \tau^2}, \quad (2)$$

$$\tau(t) = \frac{t - t_0}{t_E}. \quad (3)$$

The impact parameter u is the angular separation between the source and lens measured in units of the angular Einstein radius,

$$\theta_E = \sqrt{\frac{4GM D_{LS}}{c^2 D_L D_S}}, \quad (4)$$

where M is the mass of the lens, D_S is the observer-source distance, D_L the observer-lens distance, D_{LS} the source-lens distance and u_0 is the impact parameter at t_0 , the time of maximum magnification. The Einstein radius crossing time,

$$t_E = \frac{\theta_E}{\mu_{\text{rel}}}, \quad (5)$$

where μ_{rel} is the relative proper motion between the lens and source.

The lightcurve of a PSPL event can thus be characterised by $3 + 2n$ parameters, (t_0, u_0, t_E) plus for each n telescope + filter combinations, the unmagnified (baseline) magnitude of the source star m_{base} and the blending parameter f_{bl} , where $1 - f_{\text{bl}}$ is the fraction of blended (non-lensed) light. The maximum magnification, $A_0 = A(u_0)$ frequently replaces u_0 as a parameter.

The conventional method for predicting peak magnifications is to use χ^2 minimization techniques to fit PSPL models to data from OGLE III (possibly supplemented by a follow-up group’s own data) as they become available. Such fits are continuously updated and the subsequent predictions revised as data accumulate. Experience has shown that early predictions of eventual maximum magnification using these methods systematically yield overpredictions, strongly limiting the usefulness of such estimates. In particular, very large maximum magnifications (with large uncertainties) are often predicted for events that turn out to be of rather low amplitude. Valuable observing time is often wasted monitoring such events in order to confirm their nature.

The reason for this overprediction of values for A_0 is that in using χ^2 minimization for a predictive purpose, one implicitly assumes that all parameter values are equally likely. However, for microlensing events this is far from being the case. From a purely geometrical perspective, high magnification events are exceedingly rare. In practice, being of high magnification, they have a higher probability of detection by a survey group. It is the individual detection efficiency of a survey convolved with the intrinsic event rates (both of these as a function of event parameters) that determines the magnification probability, given that an event has been detected.

These ideas can be given a quantitative basis in a Bayesian formulation of the problem. The merits of the Bayesian approach to statistical analysis have been discussed at length elsewhere and will not be reargued (Loredo 1990; Sivia 1996). Here we simply note that a Bayesian formulation with appropriate priors should produce an unbiased estimate of the eventual microlensing event parameters during the rising part of a lightcurve.

From Bayes’ theorem, the probability density for a microlensing event to have a certain set of parameter values $\underline{\theta}$, given the fact, O , that it has been detected by the OGLE III EWS

and that data D have been acquired,

$$p(\underline{\theta}|D, O) \propto p(D|\underline{\theta}, O) p(\underline{\theta}|O), \quad (6)$$

where $\underline{\theta} = (A_0, t_E, t_0, m_{\text{base}}^j, f_{\text{bl}}^j, j = 1..n)$. The second term on the right hand side of equation (6), $p(\underline{\theta}|O)$ (known as the prior), is the underlying probability density for $\underline{\theta}$ given a detection, i.e. $p(\underline{\theta}|O)d\underline{\theta}$ is the probability that $\underline{\theta}$ is in the range $[\underline{\theta}, \underline{\theta} + d\underline{\theta}]$. It is this function that incorporates both the natural event occurrence probability and the particular parameter sensitivities of the detection system. The first term, $p(D|\underline{\theta}, O) = \mathcal{L}(\underline{\theta}|D)$, the likelihood function for $\underline{\theta}$ given D . Data from the OGLE III survey consist of I -band magnitudes and their uncertainties (m_i, σ_i) at time t_i (i.e. $n = 1$). I assume each m_i to be drawn randomly from a normal distribution $N(m_{i,0}, \sigma_i)$ where the true value of the magnitude at time t_i is $m_{i,0}$. This implies that

$$\mathcal{L}(\underline{\theta}|D) \propto e^{-\chi^2/2} \quad (7)$$

where

$$\chi^2 = \sum_i \left(\frac{m_i - m(t_i, \underline{\theta})}{\sigma_i} \right)^2, \quad (8)$$

and $m(t_i, \underline{\theta})$ is the magnitude evaluated from the model parameterised by $\underline{\theta}$.

Analogous to a χ^2 minimization, the value of $\underline{\theta}$ that maximises $p(\underline{\theta}|D, O)$ (i.e. the posterior mode) is taken as the best estimator of $\underline{\theta}_0$, the true value of $\underline{\theta}$. In the absence of a prior, this solution reduces to the minimum χ^2 solution. We stress here that when sufficient data are available to constrain a fit to a certain event, e.g. when the event is over, the Bayesian and χ^2 minimization techniques give the same parameter values and the choice of prior is largely irrelevant. In other words, the solution is not driven by prior probabilities when sufficient empirical information is available (see Sivia 1996, Chapter 2 for a discussion of this point).

If the parameters $\underline{\theta}$ are statistically independent quantities¹, $p(\underline{\theta}|O)$ factorizes as

$$p(\underline{\theta}|O) = p(A_0) p(t_E) p(t_0) p(m_b) p(f_{\text{bl}}), \quad (9)$$

where for brevity I have omitted " $|O$ " in the probability densities on the right hand side of the equation. It is often more convenient to work in decadic logarithmic units for several of these quantities, in which case

$$p(\underline{\theta}|O) = \frac{p(\lg A_0) p(\lg(t_E/t^*)) p(\lg(\Delta t_0/t^*)) p(m_b)p(f_{\text{bl}})}{(\ln 10)^3 A_0 (t_E/t^*) (\Delta t_0/t^*)}, \quad (10)$$

¹This is not necessarily the case given that a detection system may preferentially select events with parameter correlations, however inspection of EWS-detected events has not revealed any such correlations as yet.

with t^* being an arbitrary unit of time. Here I define Δt_0 to be the time to peak magnification from an initial “alert date”. For the remainder of this paper I adopt $t^* = 1$ d.

It is worth noting that even if each parameter in $\underline{\theta}$ is independent in $p(\underline{\theta}|O)$, they are not independent in the likelihood function $p(D|\underline{\theta}, O)$ and hence not independent in $p(\underline{\theta}|D, O)$. Thus when fitting a model to a lightcurve, particularly when only early data are available, the fitted maximum magnification is affected not only by the prior on A_0 but also by the priors on the other other parameters.

2.1. Inclusion of a blending parameter

The criterion used by the OGLE III EWS is that a blending parameter is only used when it is more than $3\text{-}\sigma$ less than unity and is larger than its formal uncertainty. In this paper I use the odds ratio test, a natural way to decide between two different models. I define the odds ratio

$$\frac{p(\tilde{\underline{\theta}}|D, O)}{p(\underline{\theta}|D, O)} = \frac{p(D|\tilde{\underline{\theta}}, O) p(\tilde{\underline{\theta}}|O)}{p(D|\underline{\theta}, O) p(\underline{\theta}|O)}, \quad (11)$$

where $\tilde{\underline{\theta}} = (A_0, t_E, t_0, m_{\text{base}}^j, j = 1..n)$ indicates the set of model parameters without blending ($n = 1$ when considering only EWS data). Having no *a priori* indication about whether to include blending I choose $p(\tilde{\underline{\theta}}|O) = p(\underline{\theta}|O)$. If we assume a uniform prior probability density for f_{bl} in the range $0 < f_{\text{bl}} \leq 1$ and zero outside this range, and assuming a Gaussian probability density function for f_{bl} about $f_{\text{bl},0}$, it can be shown (see for instance Sivia 1996 Ch 4) that equation (11) reduces to

$$\frac{p(\tilde{\underline{\theta}}|D, O)}{p(\underline{\theta}|D, O)} = \frac{p(D|\tilde{\underline{\theta}}_0)}{p(D|\underline{\theta}_0)} \frac{1}{\sqrt{2\pi}\sigma_{f_{\text{bl}}}} \quad (12)$$

for cases in which $f_{\text{bl},0}$ is more than several $\sigma_{f_{\text{bl}}}$ away from the cutoffs imposed by the prior. Otherwise, for $f_{\text{bl},0}$ close to 1, equation (11) becomes

$$\frac{p(\tilde{\underline{\theta}}|D, O)}{p(\underline{\theta}|D, O)} = \frac{p(D|\tilde{\underline{\theta}}_0)}{p(D|\underline{\theta}_0)} \frac{1}{\sqrt{\frac{\pi}{2}}\sigma_{f_{\text{bl}}}} \left(1 + \text{erf} \left(\frac{1-f_{\text{bl},0}}{\sqrt{2}\sigma_{f_{\text{bl}}}} \right) \right), \quad (13)$$

while for $f_{\text{bl},0}$ close to 0

$$\frac{p(\tilde{\underline{\theta}}|D, O)}{p(\underline{\theta}|D, O)} = \frac{p(D|\tilde{\underline{\theta}}_0)}{p(D|\underline{\theta}_0)} \frac{1}{\sqrt{\frac{\pi}{2}}\sigma_{f_{\text{bl}}}} \left(1 + \text{erf} \left(\frac{f_{\text{bl},0}}{\sqrt{2}\sigma_{f_{\text{bl}}}} \right) \right). \quad (14)$$

The odds ratio is then made up of two terms. The first of these represents a relative “goodness of fit” between the two models while the second is the “Occam penalty” for introducing a

new parameter. Only when $f_{\text{bl},0} < 1$ and the odds ratio is less than unity is a blending parameter used in this analysis.

3. Statistical properties of the 2002 OGLE events

I have used the set of microlensing events detected by the EWS in 2002 to determine the parameter priors. Since our interest is in the set of PSPL events, I have removed 41 events that showed deviations from PSPL behavior from this analysis. Excluded events were numbered 18, 23, 40, 51, 68, 69, 77, 80, 81, 99, 113, 119, 126, 127, 128, 129, 131, 135, 143, 149, 159, 175, 194, 202, 203, 205, 215, 228, 229, 232, 238, 254, 255, 256, 266, 273, 307, 315, 339, 348, 360, out of the complete set of 389 alerts.

Parameter values have been obtained for these events using a simplex downhill method to minimise χ^2 (EWS estimates of A_0 , t_E , m_b , f_{bl} can also be obtained from the EWS web page). For Δt_0 we require an objective definition of an “alert date” that can be applied to all events. I have arbitrarily chosen a working definition of an alert date as being the date at which three successive data points have been more than $1\text{-}\sigma$ brighter than m_b , the baseline magnitude. In practice, m_b can be determined separately from and in advance of the other parameters.

The distributions of $\lg A_0$, $\lg t_E$ and $\lg \Delta t_0$ are shown in Figure 1. For the purposes of obtaining Bayesian prior probability densities for these quantities, the distribution functions are adequately represented by the following empirically-chosen functions, also shown in Figure 1:

$$p(\lg A_0) = 0.660 \exp[-1.289 \lg A_0] \quad (15)$$

$$p(\lg(t_E/t^*)) = 0.476 \exp[-(\lg(t_E/t^*) - 1.333)^2/0.330] \quad (16)$$

$$p(\lg(\Delta t_0/t^*)) = 0.156 \exp[-(\lg(\Delta t_0/t^*) - 1.432)^2/0.458]. \quad (17)$$

It is also instructive to examine the distribution of u_0 , shown in Figure 2(a). In the absence of any selection effects, this distribution should be uniform. In fact, there is an enhanced sensitivity to detection of high magnification (low u_0) events and a rapid decrease in sensitivity for $u_0 \gtrsim 0.85$. Figure 2(a) also shows the shape of the adopted prior on $\lg A_0$ (eq. 15) when transformed to u_0 .

Figure 2(b) shows the same data but excluding those events where A_0 has a formal uncertainty greater than 50%. This illustrates that many high amplification events have maxima that are poorly constrained from OGLE data alone.

4. Application to 2003 OGLE alerts

As a test of the Bayesian method, I have applied a fitting procedure that maximises $p(\underline{\theta}|D, O)$ to a sample of the PSPL events alerted in real time by the OGLE III EWS in 2003. These consist of events OGLE-2003-BUL-138 to OGLE-2003-BUL-462 and excluding events numbered 145, 160, 168, 170, 176, 192, 200, 230, 236, 252, 260, 266, 267, 271, 282, 286, 293, 303, 306, 311, 359, 380, 419 that do not appear to be due to PSPL microlensing and 188, 197, 245, 263, 274, 297, 387, 399, 407, 412, 413, 417, 420, 422, 429, 430, 432, 433, 435, 437, 440, 441, 442, 443, 444, 449, 450, 452, 453, 454, 455, 457, 459, 461, 462 that were still ongoing at the time of writing. Events OGLE-2003-BUL-137 and earlier were announced by the EWS in a single email at the beginning of the 2003 Bulge season and thus not alerted in real time. OGLE-2003-BUL-238 (A. Gould 2004, private communication) and 262 (Yoo et al. 2004) are events in which the lens is known to have transited the source and OGLE-2003-BUL-208 and 222 may also involve finite source effects. These events have not been excluded. For the remaining sample of 267 events, I have used only the OGLE III data taken before the EWS alert time, defined as the reception of the alert email by the author. For the zero point of Δt_0 for each event, I have used the definition in § 2 except for cases in which this has not occurred before the EWS alert time in which case the latter has been used as the zero point.

As mentioned in § 1, different fitting codes can produce different estimates of maximum magnifications, particularly for high-magnification events for which blending may be involved. In particular, there is a concern that a direct comparison of predictions with the EWS alert predictions may suffer from such differences. In order to compare the maximum magnifications predicted by the Bayesian method with those predicted using χ^2 fitting, I have thus used very similar computer codes to make $p(\underline{\theta}|D, O)$ and χ^2 optimisations, electing not to use the EWS-fitted parameters. To avoid the problem of slightly different blending parameters resulting in large differences in derived magnifications, for each event I compute the brightness increase, $\Delta m = m_{\text{base}} - m(t_0)$, where $m(t_0)$ is the magnitude at t_0 . The predicted values of Δm using only the pre-alert data for an event are compared with the values determined using all the data. When all the data are available, the parameters derived using χ^2 and $p(\underline{\theta}|D, O)$ are almost always identical. Exceptions to this are in a few cases for which there are no data over the peak to constrain the fits.

4.1. Comparison of Bayesian and χ^2 predictions

The predictive performances of the Bayesian and χ^2 models at the time of EWS alert are illustrated in Figures 3 – 5. Figure 3 shows the distributions of predicted peak magnifications for both models and compares these with the eventual values. Figure 4 shows the

same data as a function of u_0 . For the χ^2 models, there is clearly a population of low u_0 events with predicted brightenings of more than 10 magnitudes that do not eventuate. Such overpredictions are not present in the Bayesian fitted models. On the other hand, there is a tendency for the Bayesian models to underpredict the peak, and at alert time to fail to predict the small population of high magnification events in Figure 3(a). In Figure 5 I compare the distribution of the differences in predicted vs actual brightenings for both models. Again, the tendency for the χ^2 fits to overestimate the peak is obvious.

5. Case studies

As pointed out in § 4.1, Bayesian solutions to early lightcurve data often fail to indicate the nature of high magnification events. It would be of concern if high magnification events were not observed due to this tendency. To illustrate in more detail the behavior of Bayesian vs χ^2 models, I consider here examples of low and high magnification events. These examples show several generic aspects of how Bayesian vs χ^2 solutions evolve as data accumulate.

OGLE-2003-BLG-171 was a low magnification event ($A_0 = 1.37$). At this magnification, the source star barely passes within one Einstein radius of the lens and the event is unsuitable for detecting a planetary anomaly. This is typical of the type of event that a follow-up program should avoid observing. Figure 6 shows χ^2 and Bayesian fitted lightcurves at 5 day intervals as the event evolves from its alert date. The predicted maximum magnifications corresponding to each panel are listed in Table 1. At alert, the event is predicted to be of low magnification but by JD 2452785 (panel d in Fig. 6), the χ^2 solution suggests a high magnification, albeit with a large uncertainty. Since the lightcurve appears to be rising rapidly, follow-up programs may well begin observing the event in order to improve on the high uncertainty in the predicted peak magnification. As more data accumulate, the low-magnification nature of the event becomes apparent. Although the true nature of the event would be identified relatively quickly by a follow-up observing program, there is a not-insignificant overhead associated with adding the event to the program. In contrast to the χ^2 fit, the predicted peak magnification for the Bayesian solution changes steadily with time. At no time is a high-magnification event suggested and a follow-up strategy based on this method would ignore the event.

OGLE-2003-BLG-208 (Fig. 7, Table 2) reached a moderately high magnification ($A_0 \approx 45$, $A_{0,\text{unblended}} \approx 17$). The projected source trajectory passed as close as $0.02 \theta_E$ to the lens and thus had a high probability of intersecting a central caustic if it were present. The alert date for this event corresponds to panel (c) in Figure 7 at which time the predictions of peak magnification are 2×10^5 and 4.4 for the χ^2 and Bayesian solutions respectively. The

Bayesian prediction of $A_0 = 4.4$ is sufficiently high to warrant the attention of a follow-up observing program such as PLANET. As data accumulate, the χ^2 predicted peak magnification rises until reaching 5×10^6 in panel (g). The true peak magnification ($A_0 \simeq 48$) starts to become apparent from panel (h) as the event peaks. In contrast, the Bayesian predicted peak magnification rises steadily until the true peak magnification is identified from around the time of panels (f) – (g).

The behavior illustrated by these two examples is typical. For low magnification events, the Bayesian model never indicates them as being worthy of observational follow-up. For high magnification events that should be observed, the peak magnification is initially underestimated but adjusts to an appropriate prediction as soon as the data indicate. In all cases examined, this occurs relatively early in the event when the magnification, $A \lesssim 3$. For both high and low magnification events, the Bayesian predicted peak magnification changes smoothly while the χ^2 prediction is prone to large changes as new data points are included. The Bayesian solutions usually converge to the correct amplification earlier than the χ^2 solutions.

6. Summary

High magnification events provide the best opportunity for detecting signals of planets around lens stars and for obtaining upper limits on their abundances. Intensive photometric monitoring programs are hampered currently by difficulties in identifying high magnification events well before peak. Systems that use χ^2 minimization to fit PSPL models to early data are prone to exaggerated predictions of peak magnification. Such predictions induce observers to spend their time monitoring events that ultimately have little statistical power.

I have shown here that a predictive system based on a Bayesian formalism that takes account of the characteristics of a detection system is immune to such behavior. Although such a Bayesian system tends to initially underpredict the peak for high magnification events, accurate prediction occurs as soon as sufficient data accumulate to justify the assertion. In all cases examined, this occurs well ahead of peak in their associated lightcurves and early enough for the events to be targeted for observation. Implementation of such a system based on the OGLE Early Warning System should result in much improved observing productivity for the 2004 season.

I am grateful to Martin Dominik for his comments on an earlier version of this paper. I think the referee, Andy Gould, for his suggested improvements to the manuscript. This work was supported by the Marsden Fund under contract UOC302.

REFERENCES

- Albrow, M.D., et al., 1998, *ApJ*, 509, 687
- Albrow, M.D., et al., 2001, *ApJ*, 556, 113
- Alcock, C., et al., 1993, *Nature*, 365, 621
- Alcock, C., et al., 1995, *ApJ*, 445, 133
- Alcock, C., et al., 1997a, *ApJ*, 479, 119
- Alcock, C., et al., 1997b, *ApJ*, 491, 436
- Alcock, C., et al., 2000, *ApJ*, 541, 734
- Aubourg, E., et al., 1993, *Nature*, 365, 623
- Bond, I.A., et al, 2002, *MNRAS*, 331, 19
- Dominik, M., et al, 2002, *Planetary and Space Science*, 50, 299
- Gaudi, B.S., Naber, R.M., Sackett, P.D., 1998, *ApJ*, 500, 33
- Gaudi, B.S., et al., 2002, *ApJ*, 566, 463
- Gould, A., 1994, *ApJ*, 421, L71
- Griest, K., Safizadeh, N., 1998, *ApJ*, 500, 37
- Heyrovský, D., 2003, *ApJ*, 594, 464
- Loredo, T.J., 1990, in P.F. Fougere, ed, *Maximum Entropy and Bayesian Methods*, Kluwer, Dordrecht, pp81-142
- Paczynski, B., 1986, *ApJ*, 304, 1
- Rhie, S.H., 1999, *ApJ*, 522, 1037
- Sivia, D.S., 1996, *Data Analysis*. Oxford University Press, Oxford
- Udalski, A., et al., 1992, *Acta Astron.*, 42, 253
- Udalski, A., et al., 1993, *Acta Astron.*, 43, 289
- Udalski, A., et al., 1994a, *Acta Astron.*, 44, 165

Udalski, A., et al., 1994b, *Acta Astron.*, 44, 227

Udalski, A., et al., 2000, *Acta Astron.*, 50, 1

Udalski, A., 2003, *Acta Astron.*, 53, 291

Yoo, J., et al., 2004, *ApJ*, in press, astro-ph/0309302

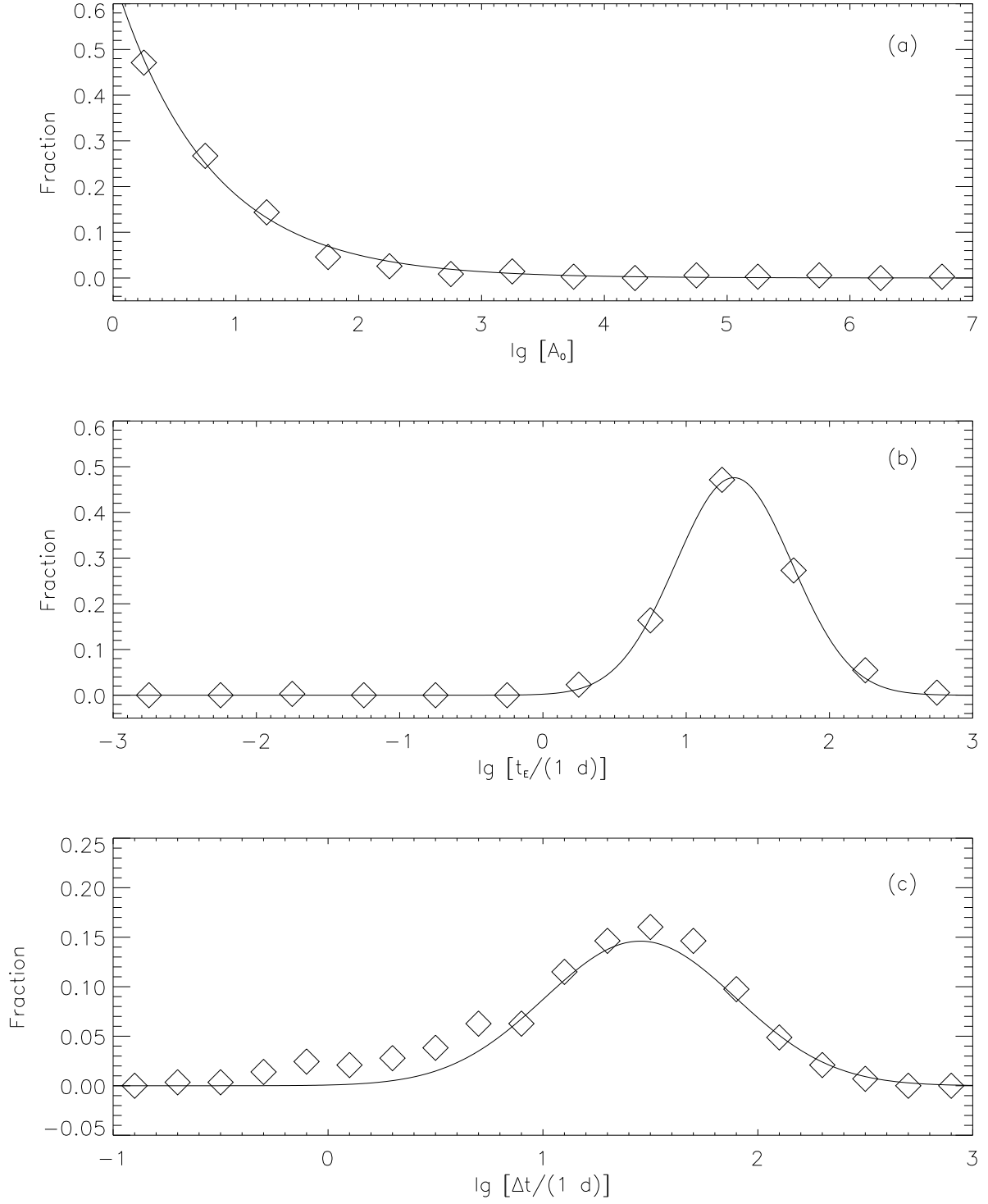


Fig. 1.— Distributions of (a) peak magnifications (b) Einstein timescales and (c) times from alert to peak magnification from my own fits to the 2002 OGLE event data. The solid lines are the adopted Bayesian priors based on these distributions.

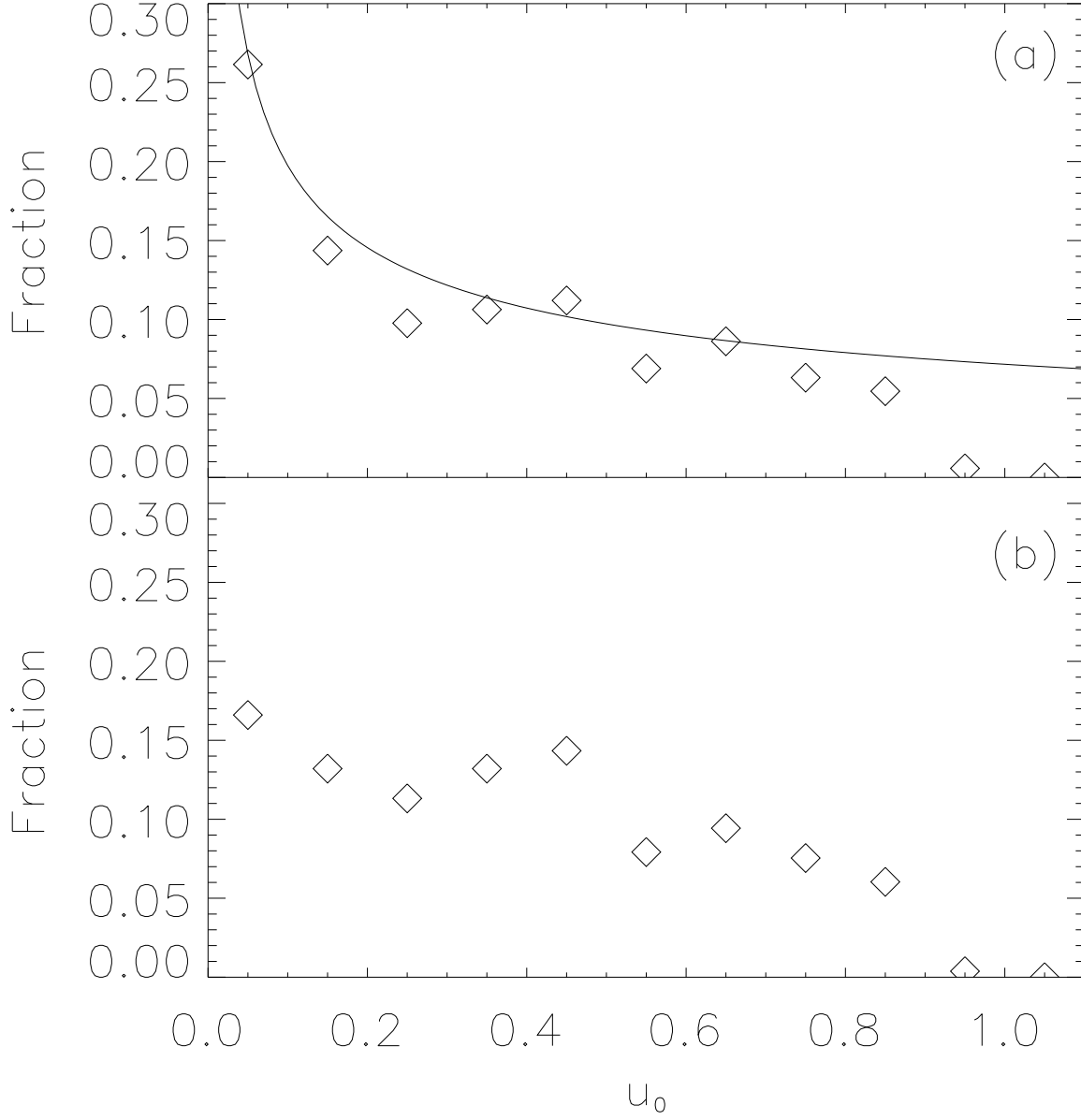


Fig. 2.— Fractional distribution of u_0 for the 2002 OGLE PSPL events. Panel (a) includes the entire data set while panel (b) excludes events for which the uncertainty in A_0 is greater than 50%. The solid line in panel (a) represents the Bayesian prior on $\lg A_0$ transformed to u_0 and scaled to the first data point.

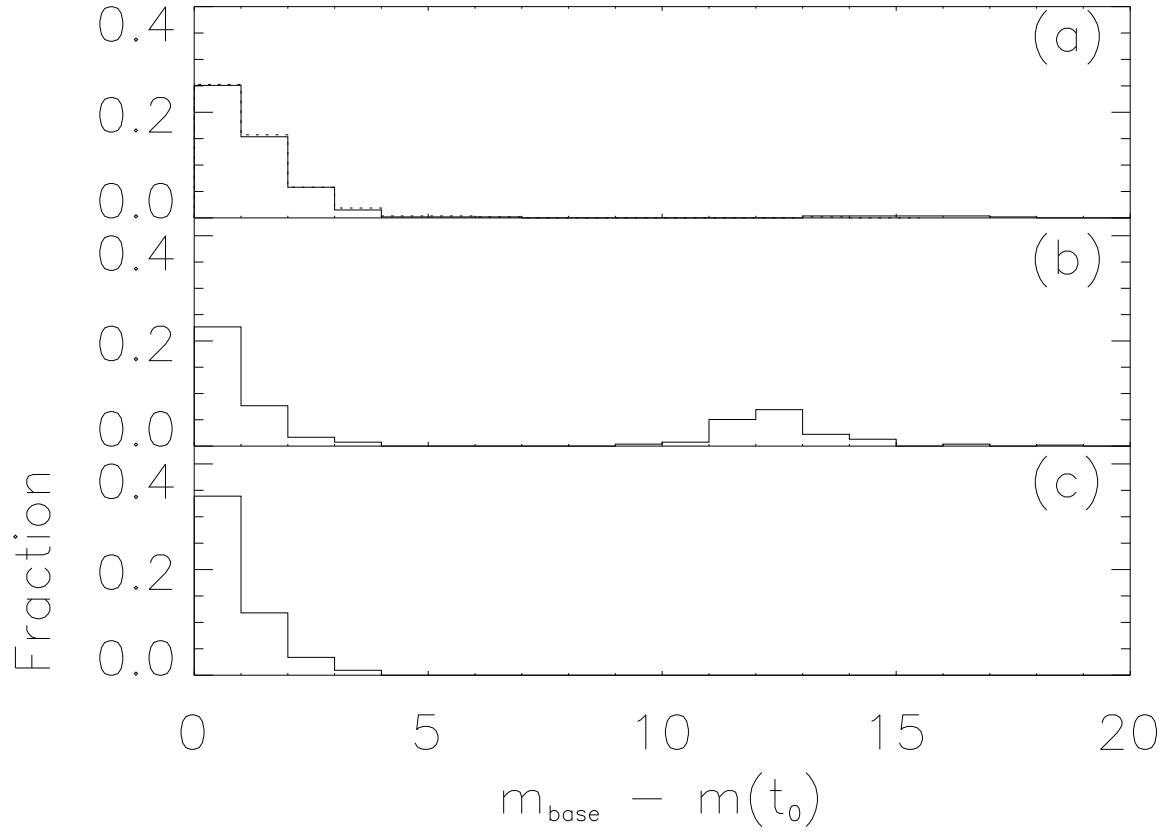


Fig. 3.— Fractional distributions of (a) OGLE peak magnifications with (b) χ^2 predictions and (c) Bayesian predictions at the time of alert. In panel (a) the solid line represents the χ^2 fits and the (mostly overplotted) dotted line represents the Bayesian fits.

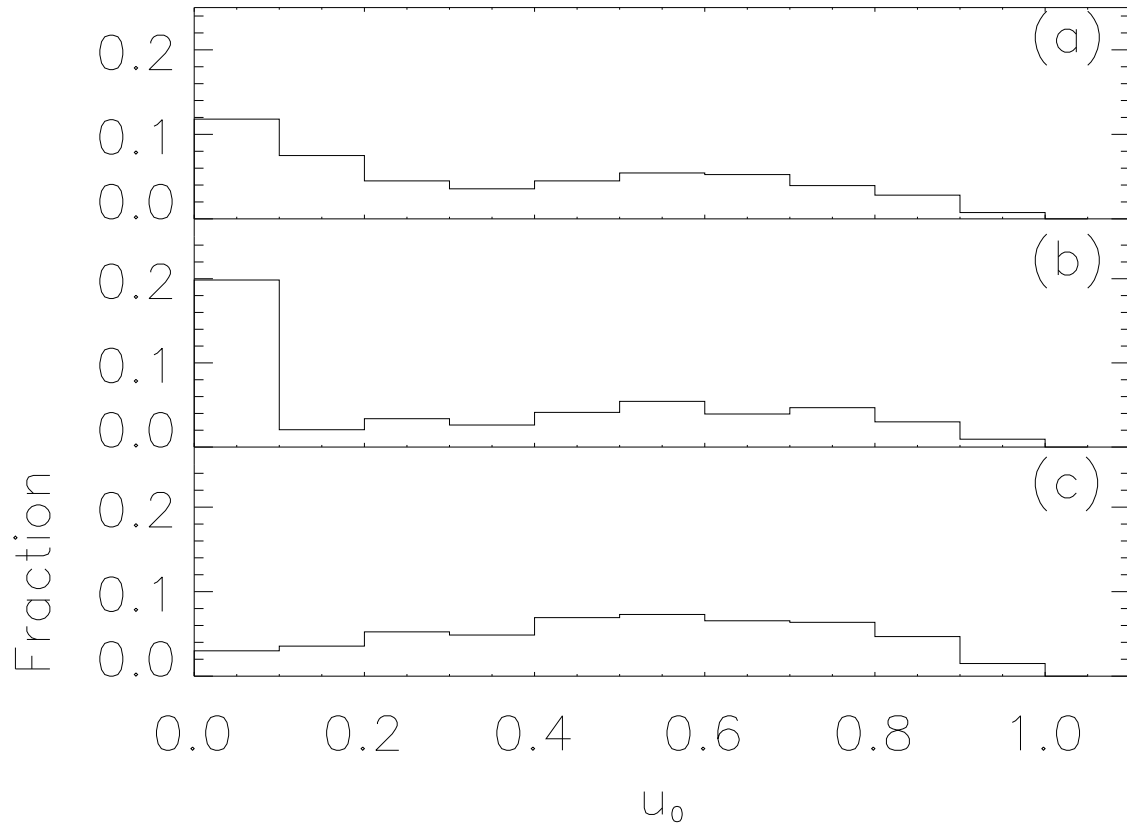


Fig. 4.— Fractional distributions of u_0 for the 2003 OGLE PSPL events. Panel (a) shows the values derived using all the data while panels (b) and (c) are respectively the χ^2 and Bayesian predictions at the time of alert.

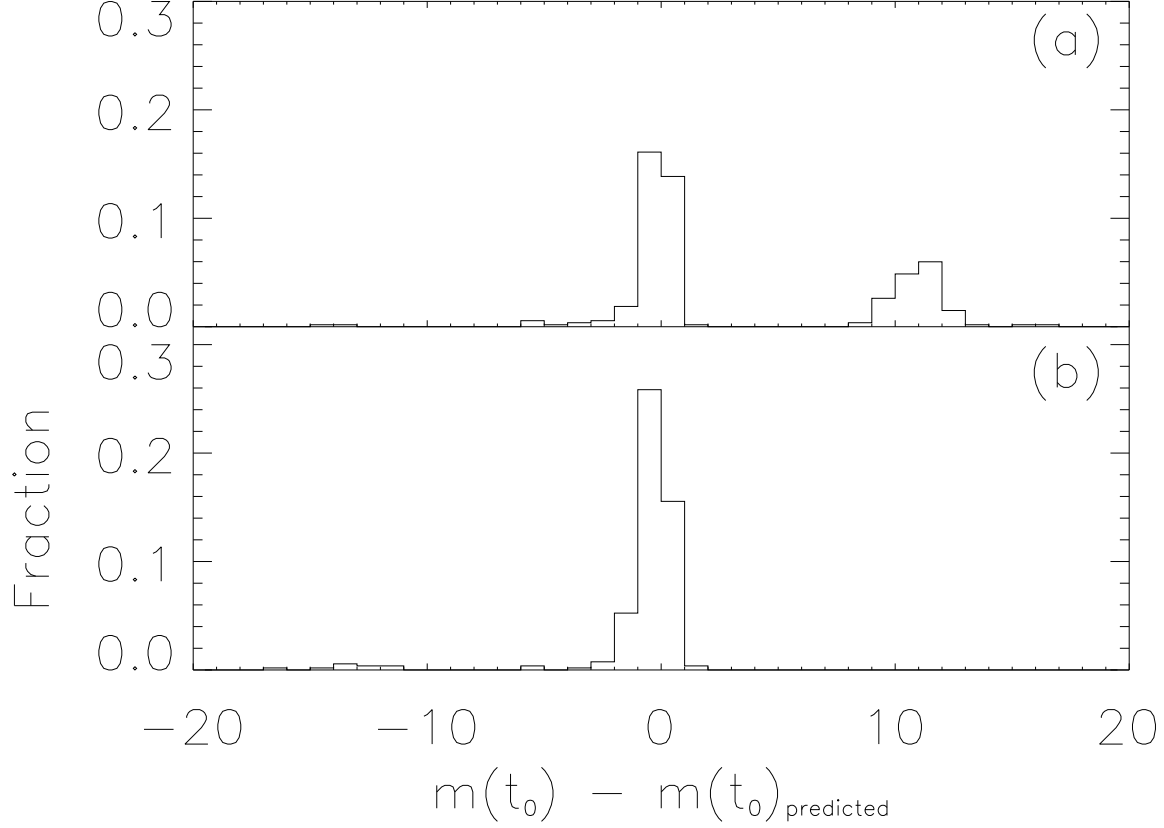


Fig. 5.— Fractional distributions of predicted peak magnitudes minus eventual peak magnitudes for (a) χ^2 and (b) Bayesian models.

Table 1. Peak magnifications for the χ^2 and Bayesian fits to OGLE-2003-BLG-171 corresponding to the panels in Figure 4.

| Panel | χ^2 | | | | | Bayesian | | | | |
|-------|-----------|------------|-----------------|--------------------------|------------------------|----------|------------|-----------------|--------------------------|------------------------|
| | A | σ_A | f_{bl} | $\sigma_{f_{\text{bl}}}$ | $A_{\text{unblended}}$ | A | σ_A | f_{bl} | $\sigma_{f_{\text{bl}}}$ | $A_{\text{unblended}}$ |
| a | 1.240 | 0.670 | 1.000 | — | 1.240 | 1.053 | 0.014 | 1.000 | — | 1.053 |
| b | 1.050 | 0.009 | 1.000 | — | 1.050 | 1.051 | 0.009 | 1.000 | — | 1.051 |
| c | 1.050 | 0.009 | 1.000 | — | 1.050 | 1.051 | 0.009 | 1.000 | — | 1.051 |
| d | 34934.748 | — | 1.000 | — | 34934.748 | 1.300 | 0.314 | 1.000 | — | 1.300 |
| e | 1.449 | 0.557 | 1.000 | — | 1.449 | 1.273 | 0.150 | 1.000 | — | 1.273 |
| f | 1.459 | 0.330 | 1.000 | — | 1.459 | 1.367 | 0.169 | 1.000 | — | 1.367 |
| g | 1.539 | 0.353 | 1.000 | — | 1.539 | 1.446 | 0.199 | 1.000 | — | 1.446 |
| h | 1.404 | 0.082 | 1.000 | — | 1.404 | 1.392 | 0.072 | 1.000 | — | 1.392 |
| i | 2.524 | 1.366 | 0.233 | 0.206 | 1.355 | 1.356 | 0.019 | 1.000 | — | 1.356 |
| j | 1.374 | 0.005 | 1.000 | — | 1.374 | 1.374 | 0.005 | 1.000 | — | 1.374 |

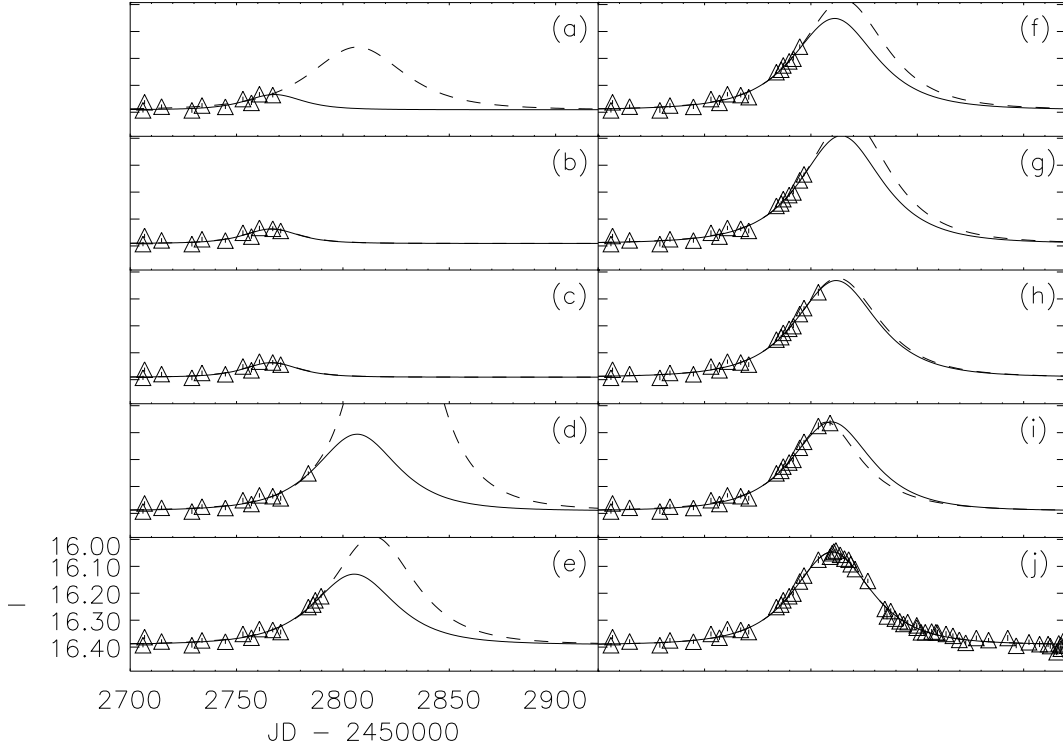


Fig. 6.— Evolution of Bayesian (solid line) and χ^2 (dashed line) fits to OGLE-2003-BLG-171. In panels (b), (c), (i) and (j) the dashed line is overprinted by the solid line. Axis ranges are the same for all panels.

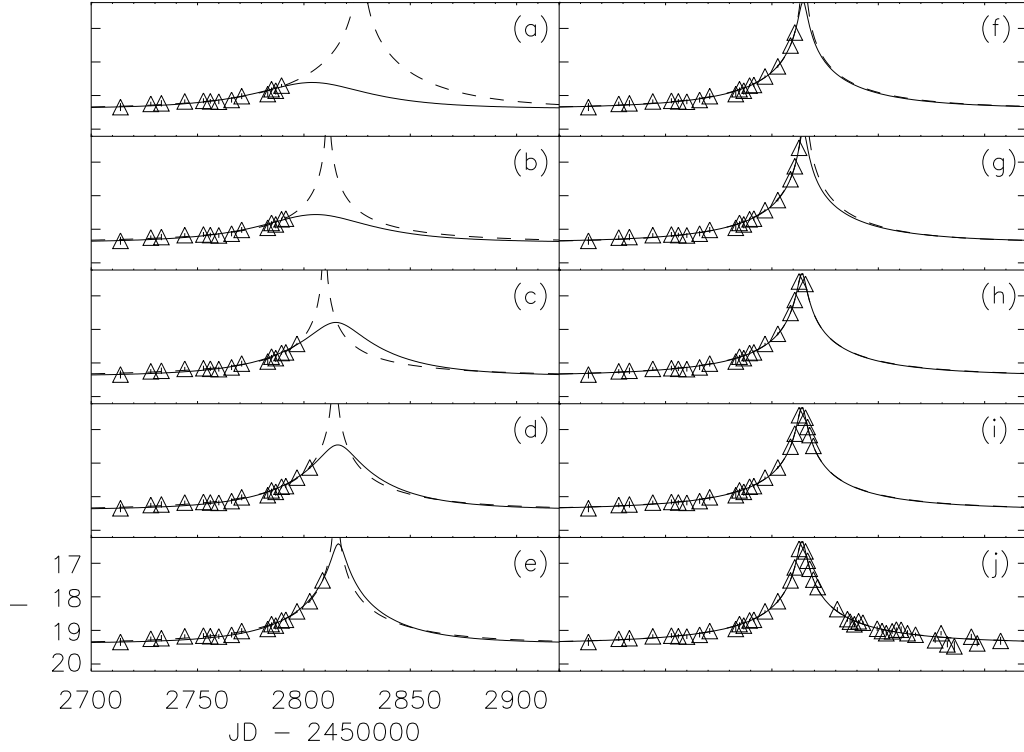


Fig. 7.— Evolution of Bayesian (solid line) and χ^2 (dashed line) fits to OGLE-2003-BLG-208. In panels (h) – (j) the dashed line is overprinted by the solid line. Axis ranges are the same for all panels.

Table 2. Peak magnifications, blend fractions and deblended peak magnifications for the χ^2 and Bayesian fits to OGLE-2003-BLG-208 corresponding to the panels in Figure 5.

| Panel | χ^2 | | | | | Bayesian | | | | |
|-------|-------------|------------|-----------------|--------------------------|------------------------|----------|------------|-----------------|--------------------------|------------------------|
| | A | σ_A | f_{bl} | $\sigma_{f_{\text{bl}}}$ | $A_{\text{unblended}}$ | A | σ_A | f_{bl} | $\sigma_{f_{\text{bl}}}$ | $A_{\text{unblended}}$ |
| a | 63601.415 | – | 1.000 | – | 63601.415 | 2.055 | 0.657 | 1.000 | – | 2.055 |
| b | 138528.609 | – | 0.209 | 0.349 | 28987.904 | 2.150 | 0.700 | 1.000 | – | 2.150 |
| c | 226215.441 | – | 0.170 | 0.168 | 38337.850 | 4.362 | 3.407 | 1.000 | – | 4.362 |
| d | 224373.536 | – | 0.382 | 0.324 | 85643.167 | 5.934 | 4.681 | 1.000 | – | 5.934 |
| e | 778431.912 | – | 0.438 | 0.232 | 340873.531 | 15.425 | 14.683 | 1.000 | – | 15.425 |
| f | 1669005.679 | – | 0.412 | 0.159 | 687516.769 | 41.122 | 31.856 | 0.452 | 0.007 | 19.150 |
| g | 4966165.089 | – | 0.586 | 0.138 | 2912064.088 | 46.816 | 12.146 | 0.456 | 0.004 | 21.888 |
| h | 55.641 | 15.221 | 0.293 | 0.076 | 17.022 | 49.816 | 1.378 | 0.326 | 0.002 | 16.893 |
| i | 53.452 | 13.513 | 0.303 | 0.073 | 16.916 | 48.446 | 1.356 | 0.333 | 0.002 | 16.813 |
| j | 48.204 | 8.750 | 0.334 | 0.056 | 16.740 | 45.814 | 1.096 | 0.350 | 0.002 | 16.661 |